Role of thermal disorder for magnetism and the α-γ transition in cerium: Results from density-functional theory

T. Jarlborg
DPMC, University of Geneva, 24 Quai Ernest-Ansermet, CH-1211 Geneva 4, Switzerland
(Received 27 March 2014; revised manuscript received 15 May 2014; published 30 May 2014)

The electronic structures of fcc Ce are calculated for large supercells with varying disorder by use of density-functional theory. Thermal disorder induces fluctuations of the amplitude of the magnetic moments and an increase in the average moments in the high-volume phase. The ferromagnetic solutions move towards a lower volume than in calculations for the perfectly ordered lattice. Therefore, disorder contributes via entropy to the stabilization of the γ phase at high T, and it is important for an understanding of the α-γ transition. Core level spectroscopy would be a means to detect disorder through the spread of Madelung shifts and local exchange splittings.

DOI: 10.1103/PhysRevB.89.184426 PACS number(s): 75.10.Lp, 64.70.K−, 65.40.−b, 71.23.−k

I. INTRODUCTION

There has been renewed interest in the isostructural α-γ transition in fcc Ce [1–8]. Ce undergoes a volume reduction of up to 17% from the magnetically disordered γ phase to a nonmagnetic (NM) low-volume α phase at low pressure P, at a temperature T of about 300 K, even though a competing double hcp (dhcp) phase β appears [9,10] at lower T for zero P. The transition moves to higher T for higher P; at ∼20 kbar it reaches almost 600 K with a vanishing volume reduction. Several models have been proposed to drive the transition, such as the Kondo volume-collapse model [11], a Mott transition [12], correlation and entropy [4,5,13], or via standard density-functional theory (DFT) bands with entropies [14,15]. The T dependence is the unusual feature of the transition. At $T = 0$ only the α phase is stable. Nevertheless, a recent work proposed that the DF potential should be replaced by a different hybrid exchange-correlation potential, with enhanced correlation, since calculations at $T = 0$ compare favorably with a measured extrapolation to a negative transition pressure [3]. There are two groups of models containing more or less correlation. Either they conclude that Ce is a strongly correlated system, where DFT is not sufficient, or otherwise they suggest that DFT is applicable, but that the band structure information has to be complemented by entropy [16,17]. In fact, DFT calculations based on the local spin-density approximation (LSDA) [18] and the generalized gradient approximation (GGA) [19] both give a qualitatively correct account of the T dependence of the α-γ transition if the entropies are included [14,15], but GGA is quantitatively better [14]. None of these DFT potentials include a particular on-site correlation beyond the normal correlation within the electron gas.

Independently of this, it has been shown that effects from thermal disorder and zero-point motion (ZPM) are important for the band structure and properties in materials with sharp density-of-states (DOS) variations near the Fermi energy (E_F). In such cases it is necessary to include disorder into the electronic structure calculations for a correct description of the physical properties or spectroscopic responses [20–23]. Magnetic manifestations of coupling between lattice distortions and electronic structures show up as spin-phonon coupling in cuprates [24] and spin-lattice interactions giving invariant thermal expansion in Invar materials [25]. Ce is, *a priori*, a system where disorder could be important, because the DOS of the f band rises sharply at E_F, and the lattice is fairly soft, which already makes large distortion amplitudes of atomic vibrations at low T. In the present paper we investigate the importance of lattice disorder for the properties of Ce and its transition between the magnetic and the nonmagnetic phase.

II. RESULTS AND DISCUSSION

A. Lattice disorder and magnetism

Self-consistent linear muffin-tin orbital (LMTO) band calculations [26] have been made for 32-atom unit cells, $2 \times 2 \times 2$ extensions of the cubic fcc 4-atom cell, of fcc Ce for several lattice constants (a_0) between 4.85 and 5.42 Å. The GGA potential is used [19]. Calculations are also made for the ordinary (ordered) fcc 1 atom/cell for a_0 between 4.75 and 5.4 Å. The number of k points is 75 in half of the Brillouin zone (BZ) for the large cell, and 505 in 1/48 BZ for the small cell. The 6s, 5p, 5d, and 4f valence electrons are included in the basis. Magnetic moments and DOS functions are very similar in these two sets of calculations for the ordered structure.

Each atomic position in the 32 atom/cell is randomly displaced in the calculations with thermal disorder so that the averaged displacement amplitudes follow a Gaussian distribution function with width σ [20]. This distribution is valid at not too large T, when there are no correlated movements of the neighboring atoms [27]. The average lattice displacement u is related to T as

$$u^2 = 3k_BT/\mathcal{M}\omega^2, \tag{1}$$

where $\mathcal{M}$ is the atomic weight and ω an averaged phonon frequency. ZPM remains at T well below the Debye temperature Θ_D and u^2 is never smaller than $3\hbar\omega/M\omega^2$ [27,28]. From the measured Θ_D of about 115 K for γ-Ce and 160 K for the high-P room temperature (RT) α phase [1] we can estimate that $\sigma_{\rm ZPM} = u_{\rm ZPM}/a_0$ is of the order 0.01–0.013, and that σ_T at RT is about 0.021–0.028 for γ and α, respectively. The band calculations are made for several disordered 32-cell configurations with σ from 0.021 up to 0.063, which corresponds to a temperature range between approximately 200 and 800 K. For comparison we note that u would be about

0.22 of the atomic sphere radius according to the Lindemann criterion for the melting temperature T_m [27], i.e., σ would be of the order 0.086. This fits with our T calibration of σ, since T_m is near 1050 K for Ce [9].

The band structure is sensitive to disorder (and ZPM) because of the fluctuations of the potential in a vibrating disordered lattice. The Coulomb potential $v_i(r)$ at a point r within a site i is

$$v_i(r) = -\sum_j Z_j/|r - R_j| + \int_0^\infty \rho(r')/|r - r'|d^3r', \quad (2)$$

where Z_j are the nuclear charges on sites j, $\rho(r)$ is the electron charge density, and the sum and integral cover all space. The contribution to $v_i(r)$ from its own site (with radius $S_i > r'$) can be separated from the contribution from the surrounding lattice through the technique of Ewald lattice summation [28]:

$$v_i(r) \approx -Z_i/r + \int_0^{S_i} \rho(r')/|r - r'|d^3r' + M_i. \quad (3)$$

Thus, the Coulomb interaction with the outside lattice is condensed into a Madelung shift M_i. This shift is identical for all sites if the lattice is perfectly ordered. But different sites have different M_i in a disordered lattice, partly because of the local differences in atomic positions and partly because of the charge transfers induced by the disorder. Thus, the potentials at different sites are slightly different and they vary in time. Phonons are very slow compared to the electronic time scale and the electronic structure can relax adiabatically. The band results for two different configurations with almost the same σ are comparable, which indicates that the 32-atom cells are large enough for a simulation of disorder. Other details of the calculational method can be found in Refs. [14,26].

Calculations for the ordered cell, and for the 1-atom fcc cell, show that a ferromagnetic (FM) ground state develops when the lattice constant a_0 exceeds about 5.2 Å [14]. The ground state solutions shift easily between a low-magnetic ($m \approx 0$) and a high-magnetic state ($m \geqslant 0.4\mu_B$/atom) when $a_0 \sim 5.3$ Å. The state at the absolute minimum of the total energy E_0 is nonmagnetic (NM), near $a_0 = 4.79$Å, compared to 4.62 Å when using LSDA [14]. The experimental values at RT are near 4.85 and 5.16 Å for the α and γ phase, respectively [9]. From the Stoner model it is expected that FM develops at a large volume, when the band narrowing makes $N(E_F)$ larger. The gain in exchange energy overcomes the loss of kinetic energy at the FM transition [29], but the Coulomb interaction can make small corrections to this energy balance [30]. These effects are included in the self-consistent, spin-polarized calculations. Structural disorder introduces local volume fluctuations, and the degree of localization of the f electrons depends directly on the surroundings. In Fig. 1 we show an example of the correlation between local volume variations ($\langle d_{\rm nn}\rangle$, which is defined as the average of the 12 nearest-neighbor distances around each of the 32 sites), and the site decomposed $N(E_F)$ values, as well as the local moments, for a case with $\sigma = 0.04a_0$, $a_0 = 5.29$ Å. As seen, when $\langle d_{nn}\rangle$ is considerably larger (>0.72) than the value for the ordered lattice (0.7071), $N(E_F)$ and m are highest. The valence charge per Ce varies quite linearly from 10.4 electron/Ce for the sites with the lowest moment to about 9.7 electron/Ce when the moment is just above $1\mu_B$/Ce. Disorder has a supplementary effect on the average moment if the lattice constant is below the critical value for a high moment: Since the local volume and the moments are increased on many of the sites with large $\langle d_{\rm nn}\rangle$, it leads to an increase of the total FM moment of the cell. That some of the sites are "compressed" (small $\langle d_{\rm nn}\rangle$) does not reduce the total moment, because their local moments are already small in the ordered lattice. Oppositely, at large a_0, when the moment for the ordered structure is close to its maximum, about $1.1\mu_B$/atom, there is no (or very little) effect on the total moment from disorder. The saturation of the total spin moment near $1\mu_B$/atom for one occupied f electron can be understood from Hund's first rule. Thus, disorder fluctuations cannot make the local moment much higher even if the local volume is increased, but local compressions could rather decrease the moment. This explains the saturation of the highest local moments seen in Fig. 1 for the sites with the highest $\langle d_{\rm nn}\rangle$ and $N(E_F)$. Figure 2 displays the averaged $m(a_0)$ for different distortion amplitudes. As seen, near the transition region there are large effects on magnetism because of lattice disorder. Magnetism appears suddenly at $a_0 \geqslant 5.3$ Å for the ordered structure, but it is much more gradual and starts at a lower volume when the disorder is large. Therefore, vibrational disorder is crucial for a good understanding of the properties of Ce.

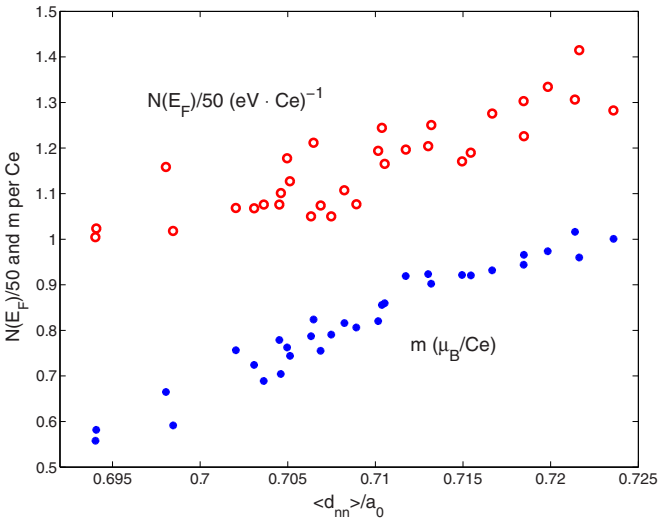

FIG. 1. (Color online) Correlation between the averaged nearest-neighbor distances $\langle d_{\rm nn}\rangle$ (in units of the lattice constant), the DOS at E_F (red open circles, in states per eV Ce/50), and local magnetic moments (blue points, in μ_B/Ce), calculated for a 32-site cell with a disorder of $\sigma = 0.04$ at the lattice constant $a_0 = 5.29$ Å. "Compressed" sites with small $\langle d_{\rm nn}\rangle$ have small $N(E_F)$ and m. Oppositely, for "isolated" sites with large $\langle d_{\rm nn}\rangle$, the $N(E_F)$ and m are the highest.

All self-consistent calculations start from the potential for the ordered structure. The final FM configurations converge gradually during the iterations. In a few cases, usually when the magnetic moments are small, it is possible to find sites where the spin orientation is opposite to the majority moments, as if antiferromagnetism (AFM) was installed locally. These solutions develop very slowly, but they do not seem to be

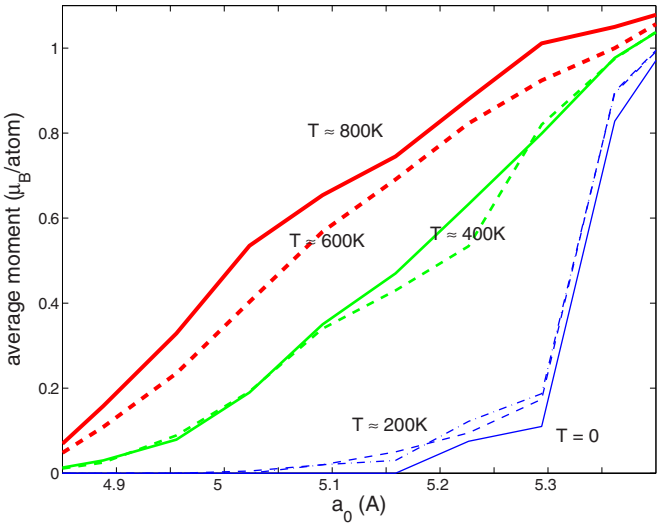

FIG. 2. (Color online) The average magnetic moment as a function of lattice constant a_0 for different levels of disorder ($\sigma = u/a_0$) between 0 ("ordered structure") and 0.063.

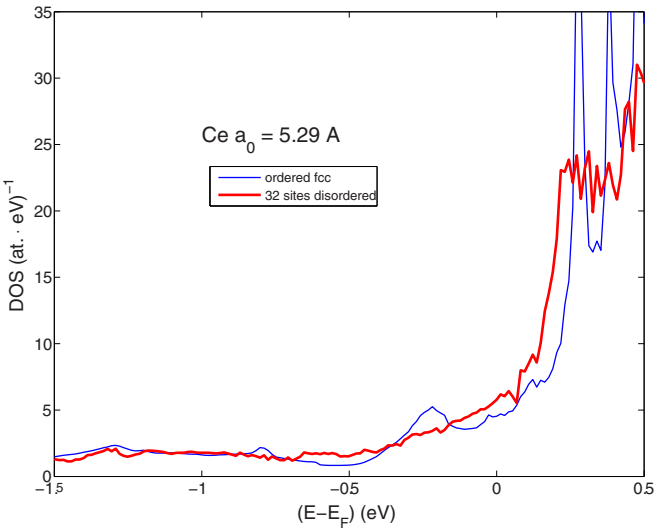

FIG. 3. (Color online) The DOS near E_F in the ordered and disordered 32 cells at the lattice constant $a_0 = 5.29$ Å. The disordered case has $\sigma = 0.04$.

concerned with large-moment cases at large volumes and large temperatures. Therefore, such solutions are not important for the free-energy arguments in the next section. The tendencies for local AFM is to diminish when the electronic temperature is raised. Thus, smearing due to the Fermi-Dirac distribution is not favorable to spin flips, while details in the local environment caused by lattice disorder can be so.

B. Free energies

Three sources of entropy were included in the GGA calculations for ordered fcc Ce [14]: vibrational, electronic, and magnetic. The difference in vibrational free energy at two volumes V_i is

$$\Delta F_{\rm vib}(V) = 3k_B T \ln\left(\frac{\Theta_\gamma}{\Theta_\alpha}\right), \tag{4}$$

where the Debye temperatures Θ_i are closely related to $\sqrt{(V_i^{1/3} B_i)}$, where B_i are the bulk moduli of the two phases. The latter are calculated to be in the range 15–20 GPa for FM Ce and 20–30 GPa for NM Ce. This agrees with experiment [1], but it is difficult to determine the full T, P dependence from *ab initio* calculations because of the sharp drop of B_i at the transition. Here we choose to fit Θ_D to the experimental results in Ref. [1]. This gives $\Theta_D \approx 160 - 22\{1 + \mathrm{sgn}(m - \frac{1}{2})\sin[\pi(m - \frac{1}{2})]^{\frac{1}{4}}\} + 15(3.54 - a_0)$ (in K). The last term makes the continuous decrease of Θ_D from about 160 K at small volumes to about 140 K at large volumes. This is the typical behavior in almost all materials, since B normally decreases with increasing volume. The second term is introduced in order to include a sharp discontinuity (∼30 K) in Θ_D at the transition when m is close to $0.5\mu_B$/atom. Thus, vibrations favor the γ phase because of its softer lattice.

The electronic entropy is calculated as

$$S_{\rm el} = -\int N(E)[f \ln f + (1 - f)\ln(1 - f)]dE, \tag{5}$$

where $N(E)$ is the electronic density of states and f is the Fermi-Dirac distribution. This quantity is almost proportional to $N(E_F)$ [$S_{\rm el} \approx \frac{2\pi^2}{3} k_B^2 T N(E_F)$], and as shown in Fig. 3, disorder makes $N(E_F)$ larger. The calculated $F_{\rm el} = E_{\rm tot} - TS_{\rm el}$ favors the γ phase even more than what was found in Ref. [14], because of disorder.

A large entropy comes from fluctuations of magnetic moments,

$$S_m = k_B \ln[2(L - m/2) + 1], \tag{6}$$

which includes an orbital moment L, and a spin part being half of the magnetic moment $m/2$. A full moment of a single f electron gives $L = 3$, according to Hund's first rule. Here we apply atomiclike Paschen-Back calculations, which for the spin-orbit coupling in Ce f give $L \approx 2.5m$ for $m \leqslant 1$ [14]. The moments L and m make a substantial entropy contribution at large T, which stabilizes the γ phase depending on the evolution of $m(T, V)$. Without considering disorder, $m(T, V)$ follows the thin solid line in Fig. 2, which is the basis for the result in Ref. [14]. As seen in Fig. 2, disorder moves the magnetic transition towards a lower volume. This fact makes the magnetic entropy contribution larger, and disorder is therefore important for the α-γ transition. Entropy from phase mixing [31] is not accounted for in the present work.

The electronic ($F_{\rm el}$) free energy is calculated from the 1 atom/cell results with T dependences entering through the Fermi-Dirac distribution and a DOS broadening. The two phases do not coexist at equal volumes. The minimum of $E_{\rm tot}$ at 4.79 Å is for NM α-Ce. FM grows gradually as $a_0 \gtrsim 5.2$ Å, but there is no second local minimum of $E_{\rm tot}$ even if there is some lowering of $E_{\rm tot}$ beyond 5.3 Å (see Fig. 4). The signature of FM, seen in the electronic free energy curve, moves to a lower volume because of higher moments when T increases. Disorder at $T \sim 400$ K makes moments appear already below $a_0 = 5$ Å.

The next step is to add the vibrational entropy and magnetic entropies from the disordered large cell calculations (scaled

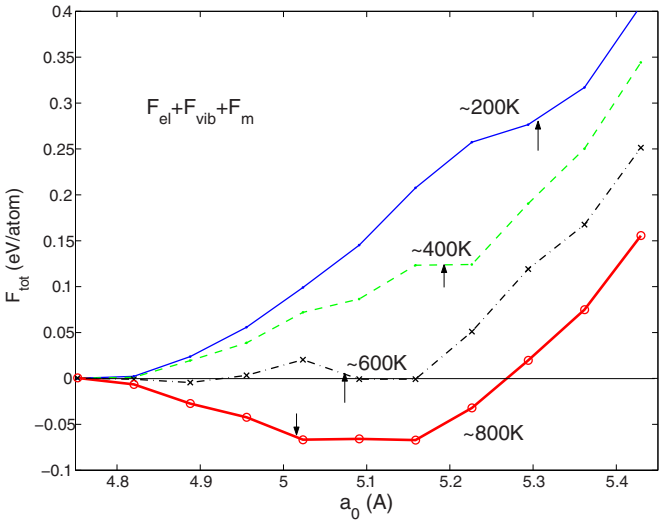

FIG. 4. (Color online) Total relative free energies ($F_{\rm tot}$ in eV/atom) as functions of the lattice constant a_0. The (blue) thin solid line shows the total free energy at low T, when the disorder is dominated by ZPM. The subsequent lines show the results at 400, 600, and 800 K, respectively. The small vertical arrows indicate the volumes where the average magnetic moment exceeds $0.5\mu_B$ per atom.

by 1/32) to the electronic free energies from the 1 atom/cell results. The results for T between 200 and 800 K are shown in Fig. 4. The crossover from the NM low-volume phase to the FM fluctuating phase at large volumes (a_0 in the range 5.1–5.15 Å) occurs just below 600 K. These results are closer in agreement with experiment than in the calculations without considering disorder [14]. The electronic total energy decreases with increasing moment, and the onset of magnetism (indicated by the arrows in Fig. 4) is seen to coincide with a small discontinuity in the $F_{\rm tot}$ curves, which moves towards a lower volume as T increases. Since the average moments in the disordered (supercell) results are higher than the moments in ordered Ce, it can be expected that the γ phase will be stabilized further.

As noted earlier, the equilibrium volume for the NM ground state is better from GGA than from LSDA. Since the crossover to the high-volume FM state occurs at a reasonable T, when using free energies from GGA, this gives us confidence that GGA is reliable also in the FM regime. Results using GGA + U (and LSDA + U) have total energies that are lower for the FM state than for the NM state already at $T = 0$ when U is large, which is incorrect [6]. Other properties such as moments and DOS at E_F seem to depend less on the exact choice of U [6], so the free-energy contribution at large T should be comparable to the present results. Thus, considering disorder and entropies in addition to GGA + U could easily destroy the good T dependence if correlation is imposed by having U larger than ∼1 eV.

C. Core levels

Core level energies are probes of potential shifts and can be used to measure the effects of disorder and magnetic fluctuations. The local variations of exchange splitting (proportional to the local magnetic moments) and Madelung shifts caused by disorder show up as a broadening of the spectroscopic ensembles of the core levels. This opens a possibility for core level spectroscopy to identify the effects of disorder. For instance, in the NM high pressure α phase at RT, disorder is calculated to make a broadening of the 4s level of about 0.16 eV. By removing the pressure (but keeping T constant) to get the magnetic γ phase, these levels broaden to about 0.42 eV because of the variations of the local moments (the averaged moment is $0.36\mu_B$/atom). Without disorder there would be no variations of the Madelung shifts, and identical exchange splittings on all sites should produce two sharp lines separated by 0.16 eV for a moment of $0.36\mu_B$/atom. The broadening from disorder is too large for a clear identification of the separated spin up and down peaks. These broadenings do not include other smearing mechanisms due to the experimental method or other types of lattice imperfections. The Madelung shifts and exchange splitting of the 4p and 4d levels are comparable, with spin-orbit splittings of 18.9 and 3.3 eV, respectively.

III. CONCLUSION

All entropies contribute to a crossover from the α to the γ phase at about 800 K when using GGA without effects from disorder [14]. Here, with disorder, the transition is calculated to occur below 600 K, at a volume in better agreement with experiment. Entropies and the effects of disorder exist always, and they should be considered even in calculations based on strong correlation. The behavior at $T = 0$ is not certain, especially because of the dhcp β phase that replaces the γ phase at low T on the $P = 0$ line [9]. Nevertheless, ignoring this and doing an extrapolation towards low T on the α-γ separation line of the phase diagram suggests a negative transition pressure at $T = 0$. This can be taken as a support for potentials with large correlation [3,5,6], but it is not clear how such results will behave at high T. Most observations of the α-γ transition are made in the range 150–450 K, and it is important to test the theoretical results in a similar temperature range. The fact that the transition can be described quite accurately by temperature dependent DFT calculations with thermal disorder and entropies is a strong support for standard DFT. Note that DFT has been applied successfully to a vast number of metallic systems without relying on adjustable parameters for correlation. Finally, Ce can be added to the list of materials where thermal disorder is seen to be important for the physical properties.

[1] M. J. Lipp, Y. Kono, Z. Jenei, H. Cynn, C. Aracne-Ruddle, C. Park, C. Kenney-Benson, and W. J. Evans, J. Phys.: Condens. Matter **25**, 345401 (2013).

[2] M. J. Lipp, A. P. Sorini, J. Bradley, B. Maddox, K. T. Moore, H. Cynn, T. P. Devereaux, Y. Xiao, P. Chow, and W. J. Evans, Phys. Rev. Lett. **109**, 195705 (2012).

[3] M. Casadei, X. Ren, P. Rinke, A. Rubio, and M. Scheffler, Phys. Rev. Lett. **109**, 146402 (2012).
[4] J. Bieder and B. Amadon, arXiv:1305.7481.
[5] N. Lanatà, Y.-X. Yao, C.-Z. Wang, K.-M. Ho, J. Schmalian, K. Haule, and G. Kotliar, Phys. Rev. Lett. **111**, 196801 (2013).
[6] F. Tran, F. Karsai, and P. Blaha, Phys. Rev. B **89**, 155106, (2014).
[7] F. Decremps, L. Belhadi, D. L. Farber, K. T. Moore, F. Occelli, M. Gauthier, A. Polian, D. Antonangeli, C. M. Aracne-Ruddle, and B. Amadon, Phys. Rev. Lett. **106**, 065701 (2011).
[8] I.-K. Jeong, T. W. Darling, M. J. Graf, Th. Proffen, R. H. Heffner, Y. Lee, T. Vogt, and J. D. Jorgensen, Phys. Rev. Lett. **92**, 105702 (2004).
[9] E. Franceschi and G. L. Olcese, Phys. Rev. Lett. **22**, 1299 (1969).
[10] W. E. Pickett, A. J. Freeman, and D. D. Koelling, Phys. Rev. B **23**, 1266 (1981), and references therein.
[11] J. W. Allen and L. Z. Liu, Phys. Rev. B **46**, 5047 (1992).
[12] B. Johansson, Philos. Mag. **30**, 469 (1974).
[13] B. Amadon, S. Biermann, A. Georges, and F. Aryasetiawan, Phys. Rev. Lett. **96**, 066402 (2006).
[14] T. Jarlborg, E. G. Moroni, and G. Grimvall, Phys. Rev. B **55**, 1288 (1997).
[15] Y. Wang, L. G. Hector, H. Zhang, S. L. Shang, L. Q. Chen, and Z. K. Liu, Phys. Rev. B **78**, 104113 (2008).
[16] O. Eriksson, M. S. S. Brooks, and B. Johansson, Phys. Rev. B **41**, 7311 (1990).
[17] Yi Wang, Phys. Rev. B **61**, R11863 (2000).
[18] W. Kohn and L. J. Sham, Phys. Rev. **140**, A1133 (1965); O. Gunnarsson and B. I. Lundquist, Phys. Rev. B **13**, 4274 (1976).
[19] J. P. Perdew and Y. Wang, Phys. Rev. B **33**, 8800 (1986).
[20] T. Jarlborg, Phys. Rev. B **59**, 15002 (1999).
[21] P. Pedrazzini, H. Wilhelm, D. Jaccard, T. Jarlborg, M. Schmidt, M. Hanfland, L. Akselrud, H. Q. Yuan, U. Schwarz, Yu. Grin, and F. Steglich, Phys. Rev. Lett. **98**, 047204 (2007).
[22] O. Delaire, K. Marty, M. B. Stone, P. R. Kent, M. S. Lucas, D. L. Abernathy, D. Mandrus, and B. C. Sales, Proc. Natl. Acad. Sci. USA **108**, 4725 (2011).
[23] T. Jarlborg, P. Chudzinski, and T. Giamarchi, Phys. Rev. B **85**, 235108 (2012).
[24] T. Jarlborg, Physica C **454**, 5 (2007).
[25] E. G. Moroni and T. Jarlborg, Phys. Rev. B **41**, 9600 (1990).
[26] O. K. Andersen, Phys. Rev. B **12**, 3060 (1975); B. Barbiellini, S. B. Dugdale, and T. Jarlborg, Comput. Mater. Sci. **28**, 287 (2003).
[27] G. Grimvall, *Thermophysical Properties of Materials* (North-Holland, Amsterdam, 1986).
[28] J. M. Ziman, *Principles of the Theory of Solids* (Cambridge University Press, New York, 1971).
[29] T. Jarlborg and A. J. Freeman, Phys. Rev. B **22**, 2332 (1980).
[30] T. Jarlborg, Phys. Rev. B **58**, 9599 (1998); Phys. Rev. Lett. **85**, 186 (2000).
[31] M. Lüders, A. Ernst, M. Däne, Z. Szotek, A. Svane, D. Ködderitzsch, W. Hergert, B. L. Györffy, and W. M. Temmerman, Phys. Rev. B **71**, 205109 (2005).